Off-center impurities in a robust ferroelectric material: Case of Li in $KNbO_3$

R. Machado, M. Sepliarsky, and M. G. Stachiotti

Instituto de Física Rosario, Universidad Nacional de Rosario, 27 de Febrero 210 Bis, (2000) Rosario, Argentina

(Received 12 July 2012; revised manuscript received 7 September 2012; published 28 September 2012)

The influence of Li impurities on the phase transition sequence of $KNbO_3$ is investigated using an atomistic model with parameters fitted to first-principles calculations. We find that the replacement of K by Li ions increases local electric dipoles due to a large Li off-centering along [001] directions. Li doping strongly affects the transition temperatures of $KNbO_3$ as a result of the coupling between the off-center Li relaxation dynamics and the macroscopic polarization of the host material. This coupling produces a decrease in the temperatures for the rhombohedral-orthorhombic and orthorhombic-tetragonal phase transitions, while the temperature of the cubic-tetragonal ferroelectric phase transition increases. The Li relaxation mechanism in the different phases of $KNbO_3$ provides a simple framework to understand the transition temperature shifts.

DOI: 10.1103/PhysRevB.86.094118 PACS number(s): 77.84.Ek, 77.80.B−

I. INTRODUCTION

The effect of off-center impurities on ABO_3 perovskite compounds has become a matter of thorough investigations during the past decades. Particular interest has been focused onto slowly relaxing, symmetry-breaking defects, which are coupled to the soft-mode order parameter. A paradigmatic case is that of Li ions substituting for K in the incipient ferroelectric $KTaO_3$. Because of the ion-radius misfit, small lithium ions take off-center positions along the six equivalent [001] orientations with a displacement as large as a quarter of the lattice constant.[1–3] The off-center displacements of lithium ions produce local electric dipole moments, which change their directions with the thermal hopping motions of Li. The effective moment of the Li dipoles is greatly increased with respect to other systems, e.g., alkali halides, owing to the large value of the dielectric susceptibility at low temperature, polarizing an extended region of host cells surrounding each defect.[2–5] In this way, depending on the Li content, various phases from dipole glasslike to ferroelectric ones can be realized. Höchli and Vugmeister have reviewed the development of research in this material up to the early 1990s[6,7] and, since then, $Li_xK_{1-x}TaO_3$ continued to be a subject of numerous investigations. In spite of that, Li-doping effects on the related ferroelectric material $KNbO_3$ are practically unknown. Even more, fundamental studies on randomly distributed dipoles with orientational degrees of freedom embedded in a *robust* ferroelectric matrix are missing.

The importance of investigating the effects of off-center impurities on systems undergoing structural phase transitions resurrects by recent findings of lead-free materials with very promising piezoelectric properties.[8] In fact, it was shown that the addition of an appropriate amount of Li ions into a ferroelectric $Na_{0.5}K_{0.5}NbO_3$ (NKN) matrix produces the enhancement of its piezoelectric and electromechanical properties. Here the role of the off-center impurities seems to be crucial, being responsible for the formation of a morphotropic phase boundary between orthorhombic and tetragonal phases.[9] Off-center impurites are important not only in alkali niobates but also in the ceramic system $Ba(Ti_{0.8}Zr_{0.2}O_3)$-$Ba_{0.7}Ca_{0.3}TiO_3$, which displays a surprisingly high piezoelectric coefficient near a tricritical triple point of its phase diagram.[10] In this piezoceramic, off-center displacements of the smaller Ca ions in the Ba site[11] seem also to be relevant.

The above discussions highlight the need to understand from a fundamental point of view the role played by off-center impurities in the structural and dynamical properties of a robust ferroelectric material. In this paper we investigate the influence of Li impurities in the phase transition sequence of $KNbO_3$ using an atomistic model with parameters fitted to first-principles calculations. $KNbO_3$ is a prototypical ferroelectric perovskite that exhibits the same sequence of phase transitions as $BaTiO_3$, transforming from the cubic (C) paraelectric to the tetragonal (T) phase at 708 K, from the tetragonal to the orthorhombic (O) phase at 498 K, and from the orthorhombic to the rhombohedral (R) phase at 263 K. The T, O, and R phases are all ferroelectric. We find that the replacement of K by Li ions generates local electric dipoles, which couple strongly to the ferroelectric host, producing shifts of the transition temperatures. These shifts can be inferred from the behavior of the relaxation dynamics of the off-center impurities in the different phases of $KNbO_3$.

II. INTERATOMIC POTENTIAL APPROACH AND COMPUTATIONAL DETAILS

While first-principles calculations have contributed greatly to the physical understanding of ferroelectric perovskites, these methods are restricted to studying zero-temperature properties. Nowadays, the combination of first-principles calculations with effective Hamiltonian[12] or interatomic potential[13] techniques offers a multiscale approach to investigate the various functional properties of ferroelectric oxides in terms of temperature, composition, and size. Both methods are able to correctly reproduce the phase sequences of many ABO_3 perovskites, although the transition temperatures have relatively large errors.

We consider in this work an interatomic potential approach based on a shell model, where the electronic polarization of the atoms is implemented via the Dick-Overhauser model,[14,15] in which an atom is considered as a charged core connected to a massless charged shell. The equilibrium distance between the core and shell is a representation of the electronic polarization of that atom. The atomic interactions are represented

by potentials between each pair of atoms in the system. The interactions between different atoms are controlled by interatomic potentials whose parameters are fitted to achieve the best possible comparison with *ab initio* calculations.

The model used in this work contains fourth-order core-shell couplings (k_2 k_4), long-range Coulombic interactions, and short-range interactions described by two different types of potentials. A Born-Mayer potential $V = Ae^{-r/\rho}$ is used for the K-O, Li-O, and Nb-O pairs, and a Buckingham potential $V(r) = Ae^{-r/\rho} + C/r^6$ is used for O-O interactions. The model parameters for $KNbO_3$ were fitted in a previous work and they are listed in Ref. 13. In the present study we determined a new interatomic potential for the Li-O pairs by adjusting its parameters to potential energy wells obtained from *ab initio* calculations. That is, no explicit experimental data had been used as input for the development of the model. The *ab initio* calculations were performed with the LAPW method, as implemented in the WIEN2K code.[16] The input information corresponded to GGA (Wu-Cohen)[17] results of the energy as function of off-center Li displacements in a $2 \times 2 \times 2$ supercell of the cubic phase.

The phase transition sequence and the dynamical properties of the material are investigated by molecular-dynamics (MD) simulations using the DL-POLY package.[18] The runs were performed employing a Hoover constant-(σ,T) algorithm with external stress set to zero; all cell lengths and cell angles were allowed to fluctuate. Periodic boundary conditions over 5000 atoms were considered. The time step was 0.4 fs, which provided enough accuracy for the integration of the shell coordinates. The total time of each simulation, after 5 ps of thermalization, was 45 ps.

III. RESULTS AND DISCUSSION

The shell model for $KNbO_3$ used in this work correctly reproduces the temperature-driven phase transition sequence of the bulk, the ferroelectric behavior of $KTa_xNb_{1-x}O_3$ solid solutions,[19] and $KNbO_3/KTaO_3$ superlattices.[20] However, the transition temperatures are not well reproduced. For that reason the results are presented here using a rescaled temperature to match the experimental Curie temperature of the bulk material. Figure 1 shows the rescaled polarization-temperature phase diagram demonstrating that the nontrivial phase transition sequence of $KNbO_3$ is correctly reproduced. Briefly, at high temperatures, the averaged polarizations P_x, P_y, and P_z are all very close to zero. As the system is cooled down, P_z acquires a value clearly different from zero, while $P_x = P_y = 0$, so the system displays a transition from the paraelectric to the ferroelectric tetragonal phase. When the temperature is further reduced, the two lower ferroelectric phases appear: the orthorhombic ($P_y = P_z$ and $P_x = 0$) and finally the rhombohedral phase with approximately equal values of the three polarization components. Regarding the transition temperatures, Fig. 1 shows that if the Curie temperature is rescaled to match the experimental value, the T-O and O-R transition temperatures are very close to the experimental values. Furthermore, the lattice parameters obtained from the model in the four phases agree with experimental values to better than 1%.

From a computational point of view, a new interatomic potential must be developed to simulate Li impurities in

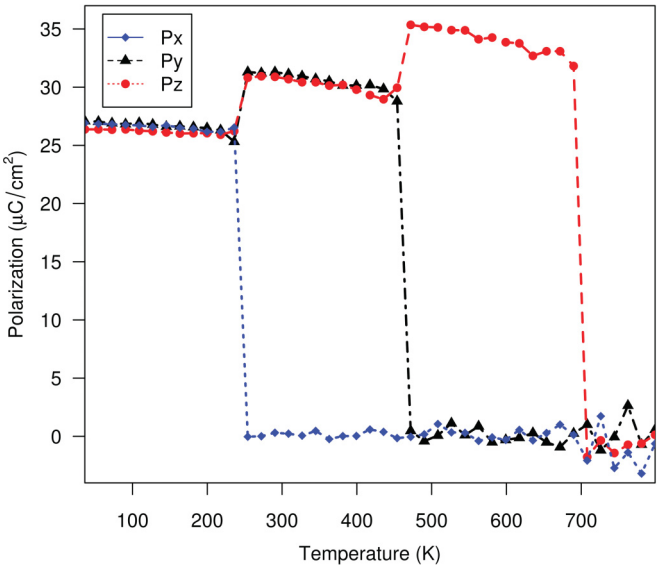

FIG. 1. (Color online) Phase diagram of $KNbO_3$ resulting from the MD simulations: the three components of the average polarization (each one represented with a different symbol) as a function of temperature. The temperature has been rescaled to match the experimental Curie temperature. The scaling factor used was 0.77.

$KNbO_3$. This new potential must be compatible with the $KNbO_3$ model in that for simulating the alloy $Li_xK_{1-x}NbO_3$ the possible difference between the two *A*-site ions lies in the different K-O and Li-O interactions and the different polarizability parameters for K and Li. We showed previously that the challenge of modeling perovskite solid-solutions with *A*-site disorder can be achieved in the framework of the shell model.[21] So, for the present study we develop a new Li-O potential by adjusting its parameters to reproduce the energetics of Li off-center displacements in $KNbO_3$ calculated from *ab initio* calculations. The fitting procedure was performed for one Li impurity in a $2 \times 2 \times 2$ supercell of the cubic phase. The energy is evaluated from an ideal *A*-site position, with all ions' coordinates frozen in the centrosymmetric positions except for Li. Figure 2 shows LAPW total energy curves for Li displacements along the [001], [011], and [111] directions. The *ab initio* calculations clearly indicate that the impurity has a strong tendency to off-centering in cubic $KNbO_3$, with energy gains of 49, 23, and 20 meV for the [001], [011], and [111] directions, respectively. The magnitude of the displacements along the three directions are 0.80 Å, 0.56 Å, and 0.52 Å. Figure 2 shows that we were able to adjust a Li-O interatomic potential, compatible with the shell model developed for $KNbO_3$, which reproduces the LAPW energetics almost quantitatively; with off-center displacements and energy reductions that are in good agreement with the *ab initio* results. The resulting parameters for the Li-O Born-Mayer potential obtained from the fitting are $A = 3571.876$ eV and $\rho = 0.211417$ Å, while the polarizability parameter for Li is $k_2 = 500$ eV/Å^2.

To check further the quality of the developed Li-O potential, a very demanding test was performed. The test consisted of simulating $LiNbO_3$, that is a system where all the K ions were replaced by Li. Surprisingly, the model for $LiNbO_3$ is able to reproduce the complex crystal structure of this compound in

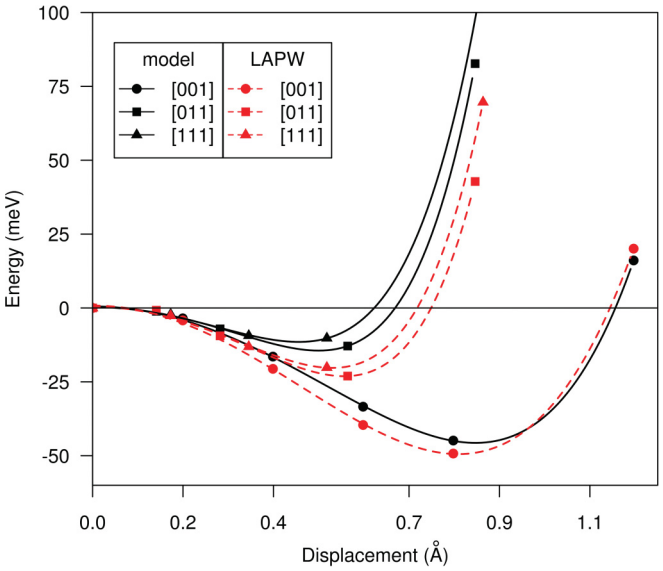

FIG. 2. (Color online) Energy as a function of Li displacement, along different crystallographic directions, from an ideal *A*-site position in $2 \times 2 \times 2$ supercell. All ions' coordinates are frozen in the centrosymmetric positions except for Li. Dotted line: LAPW. Solid line: shell model.

very good agreement with experimental results. The resulting low-temperature phase is indeed ferroelectric, with very high thermal stability, and displays a transition to a paraelectric phase at very high temperature, near the melting point. Figure 3 shows the x-ray diffraction pattern calculated for the $LiNbO_3$

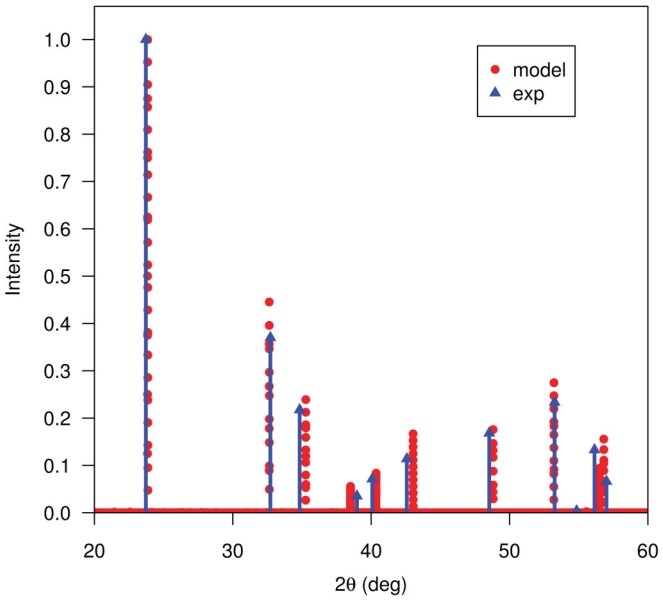

FIG. 3. (Color online) Calculated x-ray diffraction pattern for $LiNbO_3$ at room temperature generated using shell model MD simulations compared with the refined experimental structure of Ref. 22. In each case the intensities are normalized to that of the strongest peak. The configuration used for the calculation of the theoretical diffraction pattern (red points) corresponds to the time average of the lattice constants and atomic position in a $10 \times 10 \times 10$ supercell.

structure at room temperature from MD simulations. This was compared with a pattern generated using the refined structure obtained by Hsu *et al.*[22] It is clear from the figure that the diffraction pattern obtained by the MD simulations is in excellent agreement with the experimental one: the model for $LiNbO_3$ gives an rhombohedral ground state (space group R3*c*) with room-temperature lattice parameters $a = 3.742$ Å, $\alpha = 85.26°$, while the experimental results are $a = 3.764$ Å, $\alpha = 86.27°$.[22] This is a very pleasant result, which indicates that the complex R3*c* phase of $LiNbO_3$ is obtained, from the $KNbO_3$ perovskite structure, as result of oxygen octahedra rotations originated from the volume contraction due to the replacement of K by Li, plus the strong tendency of Li to off-centering.

We now examine the local structure and the dynamics of a Li impurity in the different phases of $KNbO_3$. The temperature selected for each phase is near the middle of its stability range. We considered the case of one impurity in a $10 \times 10 \times 10$ supercell, so the defect can be considered as isolated. The local structure is analyzed by the radial-distribution function $[g(r)]$ for the Li-O pairs, which are depicted in Figure 4. As it turns out, the local structure of Li is very similar in the different phases of $KNbO_3$. In fact, in all the cases $g(r)$ displays a three-peak structure, which corresponds to the 12 nearest-neighbor Li-O pairs. The integrated radial-distribution function $n(r)$ for the R phase showed in Fig. 4 indicates that each peak is originated from 4 Li-O bonds (similar graphs, not shown here, were obtained for the other phases). This is an indication that, regardless of the direction of the macroscopic polarization of the host material, Li moves off-center along [001] directions. Moreover, the peaks are centered around Li-O distances, which are similar in the different phases, indicating again that the ferroelectric host has little effect on the local structure with respect to the paraelectric phase. The magnitude of the Li off-center displacements estimated from the different

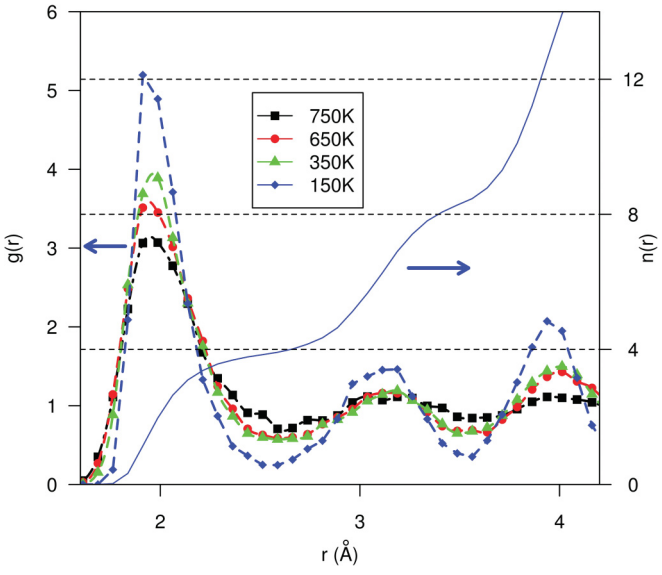

FIG. 4. (Color online) Radial-distribution function $g(r)$ for Li-O pairs in the different phases of $KNbO_3$. The integrated radial-distribution function $n(r)$ for the rhombohedral phase is showed using a thin solid line.

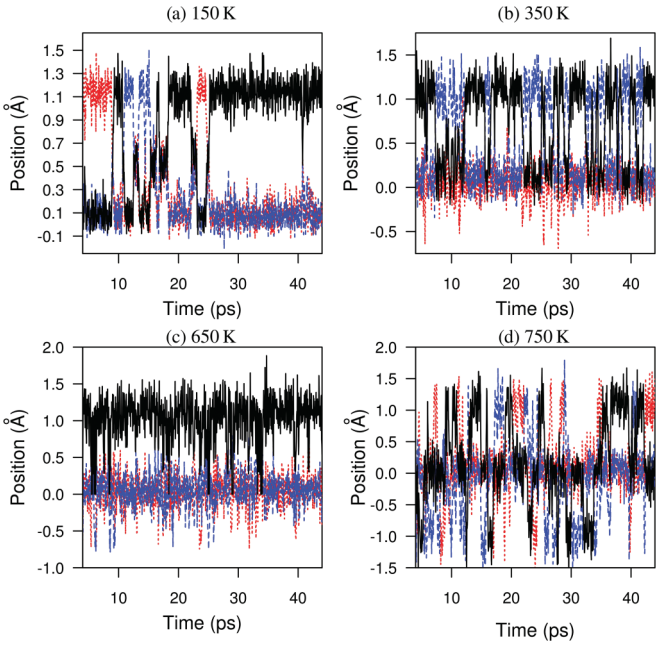

FIG. 5. (Color online) Time evolution of Li off-center displacements in the different phases of $KNbO_3$: (a) rhombohedral phase, (b) orthorhombic phase, (c) tetragonal phase, and (d) cubic phase. Dotted red, dashed blue, and solid black correspond to x-, y-, and z-displacements, respectively.

distribution functions is very similar, approximately 1.2 Å. This value is larger than 0.80 Å obtained for the supercell with all ions' coordinates frozen in the centrosymmetric positions (Fig. 2). This an indication that the magnitude of the Li displacement is very sensitive to relaxation of the surrounding ions, which is consistent with earlier results obtained for Li in $KTaO_3$.[5]

In spite of the local structure being similar in the different phases of $KNbO_3$, the impurity dynamics presents interesting particularities. Figure 5 shows the time evolution of the Cartesian coordinates of the Li ion from the ideal perovskite A-site position. In the low-temperature rhombohedral phase, the Li impurity clearly displays a relaxation dynamics between [001] off-center positions [Fig. 5(a)]. This behavior resembles the case of Li in $KTaO_3$, where the low-temperature freezing of the relaxation dynamics produces a dipole-glass phase.[6] There is, however, one important difference. While in $KTaO_3$, the impurity jumps between six equivalent off-center positions, the macroscopic polarization of $KNbO_3$ favors three of the six possibilities. That is, if the rhombohedral phase is polarized along the $[+1+1+1]$ direction, the Li ion relaxes only between the $[00+1]$, $[0+10]$, and $[+100]$ off-center positions, being forbidden the negative directions for off-centering [Fig. 5(a)]. This relaxation dynamic begins to occur well within the R phase, which is a hundred degrees below the R-O phase transition. One would expect then that the impurity relaxation perturbs the R-O transition, lowering the transition temperature (we will address this point in more detail latter). The impurity dynamics in the orthorhombic phase is similar to the previous one in the sense that Li relaxes between [001] off-center positions. However, as the orthorhombic phase is polarized along the $[0+1+1]$ direction, the relaxation process occurs between two off-center positions, $[00+1]$ and $[0+10]$ [Fig. 5(b)]. Here, again, one can speculate that the Li ions will produce a decreasing of the O-T transition temperature. In the tetragonal phase, on the contrary, the dynamics does not show any signature of relaxation [Fig. 5(a)]. In this case Li is off-center along the [001] direction, but it remains having its local dipole moment always parallel to the macroscopic polarization without hopping to another off-center position. As the local polarization of Li is stronger than the one for $KNbO_3$, the impurities reinforce the average macroscopic polarization of the alloy compound, and an increment of the T-C transition temperature with Li doping can be expected. Finally, in the cubic paraelectric phase, Li displays a relaxation dynamics between six equivalent off-center positions [Fig. 5(d)], as in $KTaO_3$. Then, each of the six positions occurs with equal probability in the course of time, resulting in vanishing local dipolar moment.

To gain more insight into the effects produced by the macroscopic polarization of the host material on the impurity dynamics, we performed supercell calculations to evaluate the energetics of off-center Li displacements in the different ferroelectric phases of $KNbO_3$. We considered the case of one Li impurity in a $5 \times 5 \times 5$ supercell to kept negligible the interaction between Li impurities situated in adjacent supercells. Since it was not feasible to optimize the geometry of this large supercell in term of all degrees of freedom, we limited ourselves to calculate the energies of off-center Li configurations keeping all ions' coordinates frozen in the positions corresponding to each ferroelectric phase. Figure 6 shows total energy curves for Li displacements along the [001] directions for the three ferroelectric phases of $KNbO_3$. Figure 6(a) shows that the macroscopic polarization of the R phase "destroy" the double-well-type potential of the cubic phase (showed in dashed lines), and only three energy minima along the [001] directions are present. Similarly, Fig. 6(b) shows total energy curves for Li displacements along the [001] directions in the O phase. In this phase, the macroscopic polarization also alters the double-well-type potential of the cubic phase in such a way that only two minima are present. We note that the two minima of the double-well-type potential along the [100] direction showed in Fig. 6(b) are indeed saddle points. Finally, Fig. 6(c) shows that only one energy minimun is obtained for Li in the tetragonal phase (the four energy minima along the [100] and [010] directions are saddle points), so a relaxational dynamics is not expected for the impurity in this case, which is in accordance with the MD results discussed above. In summary, it is clear that the underlying energy surface for the off-center displacement is strongly altered by the macroscopic polarization of the host material producing particularities in the local dynamics of Li in the different phases of $KNbO_3$.

We finally characterize quantitatively the influence of the off-center Li impurities on the phase transition sequence of $KNbO_3$ by comparing the temperature-driven phase diagram of pure $KNbO_3$ with the one obtained for a $Li_xK_{1-x}NbO_3$ alloy with low Li concentration. MD simulations were performed randomly distributing 10 Li impurities in a $10 \times 10 \times 10$ supercell, which simulates a Li concentration of 1%. The resulting lattice constants as a function of temperature are showed in Fig. 7. It is clear that the off-center impurities appreciably influence the lattice constants (the presence of Li

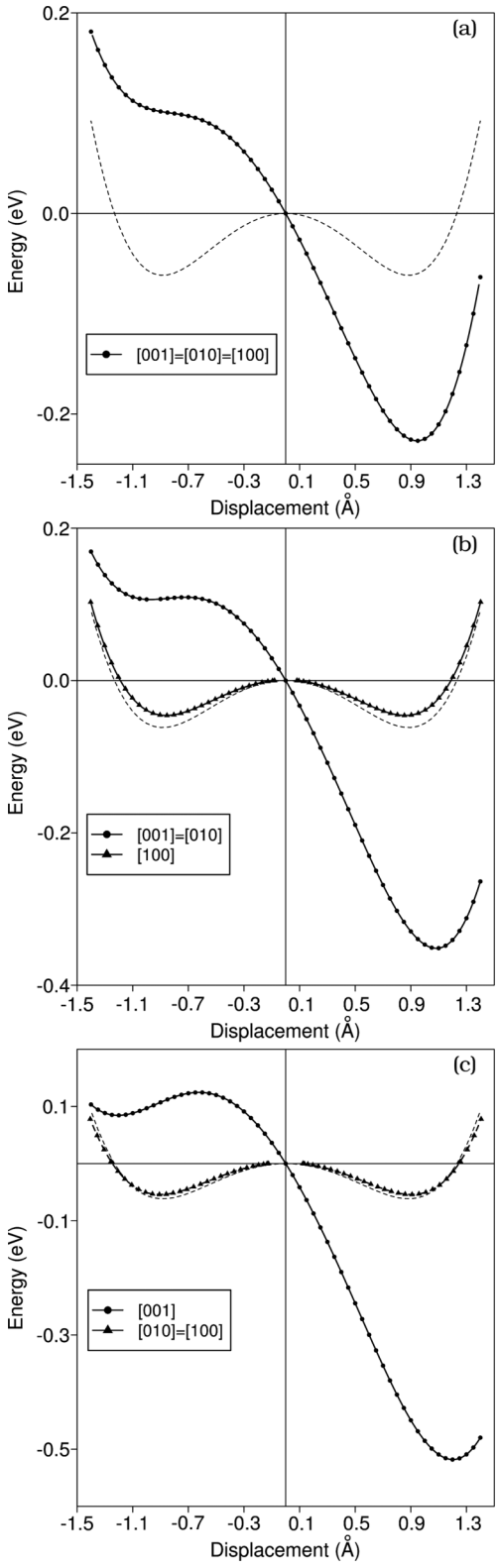

FIG. 6. Energy as a function of Li displacement, along [001] directions for the three ferroelectric phases of $KNbO_3$, from an ideal *A*-site position in $5 \times 5 \times 5$ supercell: (a) rhombohedral phase, (b) orthorhombic phase, and (c) tetragonal phase. For comparison, the "double-well-type potential" of the cubic phase is represented by dashed lines. All ions' coordinates are frozen in the positions corresponding to the ferroelectric structure of the pure material except for Li.

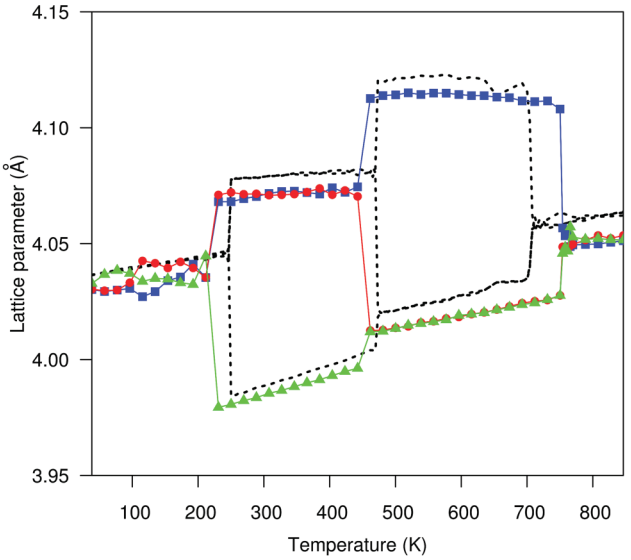

FIG. 7. (Color online) Phase diagrams of $KNbO_3$ and $Li_{0.01}K_{0.99}NbO_3$ resulting from MD simulations: cell parameters as a function of temperature. The results for $KNbO_3$ are represented by dashed lines, while the lattice parameters of $Li_{0.01}K_{0.99}NbO_3$ are represented with different symbols. The temperature has been rescaled to match the experimental Curie temperature of $KNbO_3$. The scaling factor used was 0.77.

ions at the *A* sites shrinks the cell volume) and the temperature of the phase transitions. In accordance with the predictions made previously from the relaxation dynamics of an isolated impurity, Li doping produces a decrease in the temperatures for the R-O and O-T phase transitions. On the contrary, the temperature of the C-T ferroelectric phase transition increases. These shifts, which increase with increasing Li content, are in good agreement with dielectric measurements of Li-doped $KNbO_3$ single crystals.[23] We note that the temperature shifts produce an increase of the temperature range of stability of the tetragonal phase with increasing Li content. This is consistent with first-principles investigations of $Li_{0.5}K_{0.5}NbO_3$, where a tetragonal ferroelectric ground was predicted.[24] This is significant because it suggests the possible presence of a morphotropic phase boundary between this composition and $KNbO_3$, which is rhombohedral. Even more, at a high concentration level of Li, frustration could favor the forming of a relaxor.[24] We believe that these last two points deserve a careful and detailed investigation, which is in progress.

IV. CONCLUSIONS

We have shown that the combination of first-principles calculations with shell-model techniques offers a multiscale approach to investigate finite-temperature properties of off-center impurities in ferroelectric materials. In particular, we studied the effects of Li impurities on $KNbO_3$. We showed that the developed model reveals an interesting relationship between the off-center Li impurities in $KNbO_3$ and the complex R3*c* phase of $LiNbO_3$. Regarding the temperature-driven phase transitions, we observed that the off-center defects couple strongly to the ferroelectric host, producing a decrease in the temperatures for the rhombohedral-orthorhombic and

orthorhombic-tetragonal phase transitions, while the temperature of the cubic-tetragonal ferroelectric phase transition increases. These temperature shifts, which can be inferred from the reorientation dynamics of the off-center Li impurities in each phase, produce an increase of the temperature range of stability of the tetragonal phase with increasing Li content. Our results are thus significant to better understand the microscopic behavior of Pb-free piezoelectric materials based on alkali niobates, like $Li_x(Na_{0.5}K_{0.5})_{1-x}NbO_3$.

ACKNOWLEDGMENTS

We thank Ricardo Migoni for useful discussions. We acknowledge computing time at the CCT-Rosario Computational Center. This work was sponsored by Consejo Nacional de Investigaciones Científicas y Tecnológicas (CONICET) and Agencia Nacional de Promoción Científica y Tecnológica (ANPCyT) de la Republica Argentina. M.G.S. thanks support from Consejo de Investigaciones de la Universidad Nacional de Rosario (CIUNR).

[1] J. J. van der Klink and F. Borsa, Phys. Rev. B **30**, 52 (1984).

[2] M. G. Stachiotti and R. L. Migoni, J. Phys.: Condens. Matter **2**, 4341 (1990).

[3] R. I. Eglitis, A. V. Postnikov, and G. Borstel, Phys. Rev. B **55**, 12976 (1997).

[4] M. G. Stachiotti, R. L. Migoni, and U. T. Höchli, J. Phys.: Condens. Matter **3**, 3689 (1991).

[5] S. A. Prosandeev, E. Cockayne, and B. P. Burton, Phys. Rev. B **68**, 014120 (2003).

[6] U. T. Höchli, K. Knorr, and A. Loidl, Adv. Phys. **39**, 405 (1990).

[7] B. E. Vugmeister and M. D. Glinchuk, Rev. Mod. Phys. **62**, 993 (1990).

[8] Y. Saito, H. Takao, T. Tani, T. Nonoyama, K. Takatori, T. Homma, T. Nagaya, and M. Nakamura, Nature (London) **432**, 84 (2004).

[9] Y. Guo, K. Kakimoto, and H. Ohsato, Appl. Phys. Lett. **85**, 4121 (2004).

[10] W. Liu and X. Ren, Phys. Rev. Lett. **103**, 257602 (2009).

[11] D. Fu, M. Itoh, S. Y. Koshihara, T. Kosugi, and S. Tsuneyuky, Phys. Rev. Lett. **100**, 227601 (2008).

[12] D. Vanderbilt, Curr. Opin. Solid State Mater. Sci. **2**, 701 (1997).

[13] M. Sepliarsky, A. Asthagiri, S. R. Phillpot, M. G. Stachiotti, and R. L. Migoni, Curr. Opin. Solid State Mater. Sci. **9**, 107 (2005).

[14] B. G. Dick and A. W. Overhauser, Phys. Rev. **112**, 603 (1958).

[15] M. Sepliarsky, M. G. Stachiotti, and R. L. Migoni, Phys. Rev. B **52**, 4044 (1995).

[16] P. Blaha, K. Schwarz, G. K. H. Madsen, D. Kvasnicka, and J. Luitz, *WIEN2K, An Augmented Plane Wave + Local Orbitals Program for Calculating Crystal Properties* (Karlheinz Schwarz, Techn. Universität Wien, Austria, 2001).

[17] Z. Wu and R. E. Cohen, Phys. Rev. B **73**, 235116 (2006).

[18] DL-POLY is a package of molecular simulation routines written by W. Smith and T. R. Forester, Daresbury and Rutherford Appleton Laboratory, Daresbury, UK.

[19] M. Sepliarsky, S. Phillpot, D. Wolf, M. G. Stachiotti, and R. L. Migoni, Appl. Phys. Lett. **76**, 3986 (2000).

[20] M. Sepliarsky, S. R. Phillpot, D. Wolf, M. G. Stachiotti, and R. L. Migoni, Phys. Rev. B **64**, 060101 (2001).

[21] S. Tinte, M. G. Stachiotti, S. R. Phillpot, M. Sepliarsky, D. Wolf, and R. L. Migoni, J. Phys.: Condens. Matt. **16**, 3495 (2004).

[22] R. Hsu, E. N. Maslen, D. du Boulay, and N. Ishizawa, Acta Cryst. B **53**, 420 (1997).

[23] V. A. Trepakov, M. E. Savinov, V. Zelezny, P. P. Syrnikov, A. Deyneka, and L. Jastrabik, J. Eur. Ceram. Soc. **27**, 4071 (2007).

[24] D. I. Bilc and D. J. Singh, Phys. Rev. Lett. **96**, 147602 (2006).